Impaired PTPN13 phosphatase activity in spontaneous or HPV-induced squamous cell carcinomas potentiates oncogene signaling via the MAP kinase pathway

Andrew C Hoover[1], **Gwen L Strand**[2], **Paul N Nowicki**[3], **Mary E Anderson**[1], **Paola D Vermeer**[4], **Al J Klingelhutz**[5], **Aaron D Bossler**[2], **James V Pottala**[4], **Wiljan J A J Hendriks**[6], and **John H Lee**[4,7]

[1]Department of Otolaryngology - Head and Neck Surgery, Roy J. and Lucille A. Carver College of Medicine, University of Iowa, Iowa City, Iowa 52242, USA [2]Department of Pathology, Roy J. and Lucille A. Carver College of Medicine, University of Iowa, Iowa City, Iowa 52242, USA [3]Gynecologic Oncology, Roy J. and Lucille A. Carver College of Medicine, University of Iowa, Iowa City, Iowa 52242, USA [4]Cancer Biology Research Center, Sanford Research/USD, Sioux Falls, SD 57105 USA [5]Department of Microbiology, Roy J. and Lucille A. Carver College of Medicine, University of Iowa, Iowa City, Iowa, USA [6]Department of Cell Biology, Radboud University Nijmegen Medical Centre, Nijmegen, The Netherlands [7]Sanford ENT-Head and Neck Surgery, Sanford Health, ,, Sioux Falls, South Dakota 57105, USA

Abstract

Human papillomaviruses (HPV's) are a causative factor in over 90% of cervical and 25% of head and neck squamous cell carcinomas (HNSCC's). The C-terminus of the high risk HPV 16 E6 oncoprotein physically associates with and degrades a non-receptor protein tyrosine phosphatase (PTPN13), and PTPN13 loss synergizes with H-Ras^{V12} or ErbB2 for invasive growth in vivo. Oral keratinocytes that have lost PTPN13 and express H-Ras^{V12} or ErbB2 show enhanced Ras/RAF/MEK/Erk signaling. In co-transfection studies, wild type PTPN13 inhibited Ras/RAF/MEK/Erk signaling in HEK 293 cells that over-express ErbB2, EGFR, or H-Ras^{V12}, while an enzymatically inactive PTPN13 did not. Twenty percent of HPV negative HNSCC's had PTPN13 phosphatase mutations that did not inhibit Ras/RAF/MEK/Erk signaling. Inhibition of Ras/RAF/MEK/Erk signaling using the MEK inhibitor U0126 blocked anchorage independent growth in cells lacking PTPN13. These findings show PTPN13 phosphatase activity plays a physiologically significant role in regulating MAP kinase signaling.

INTRODUCTION

Malignant transformation often occurs through random, accumulated genetic changes resulting in characteristic features shared by nearly all cancers (Hanahan and Weinberg 2000). It is estimated that viral gene expression plays a role in 20% of cancers. Viral genes frequently target key cellular pathways that are also altered in non-viral cancers. Because viral genes alter these pathways in a mechanistically consistent way, studies of their function often serve as a starting point to understanding non-viral mechanisms of transformation. In most viral cancers, synergistic cellular changes must occur for malignant progression to occur. Therefore, it is important to study viral gene function in the context of these cellular changes. The following study examines a synergy between HPV viral oncogene function and cellular changes that lead to invasion. High risk HPV's promote cancerous growth through over-expression of two multifunctional viral oncoproteins, E6 and E7. Their known transforming functions include inactivation of pRB by E7 and degradation of p53 and activation of telomerase by E6 (Longworth and Laimins 2004). E6 oncoproteins from HPV subtypes that are high risk for malignant progression also contain a C-terminal PDZ binding motif (PDZBM), which has a poorly understood yet necessary role in malignant transformation. PDZBM's are short C-terminal amino acid sequences capable of binding PDZ domain containing proteins (Jelen et al 2003). We have previously investigated the transforming effects of the E6 PDZBM of HPV type 16 in HPV related head and neck squamous cell cancers (HNSCC's) (Spanos et al 2008b) and cervical cancer (Nowicki et al, unpublished data) and have shown it physically associates with and induces loss of PTPN13, a non-receptor protein tyrosine phosphatase that contains five PDZ domains. In addition, HPV 16 E6 or shRNA mediated PTPN13 loss synergizes with H-Ras^{V12} for invasive growth in vitro and in vivo models of HNSCC (Spanos et al 2008a, Spanos et al 2008b). Besides our data, PTPN13 has been reported as a putative tumor suppressor in a wide range of epithelial cancers (including breast, colon, and hepatocellular (Wang et al 2004, Yeh et al 2006, Ying et al 2006)). Analysis of synergistic changes associated with PTPN13 loss in colon cancers showed that a majority had mutations in the MAP kinase pathway (Wang et al 2004)

Though some reports show significant association between Ras mutations and HPV in cervical cancers (Landro et al 2008, Lee et al 1996), direct activating Ras mutations (like H-Ras^{V12}) are less common in HNSCC's (Hardisson 2003, Lu et al 2006, Yarbrough et al 1994)'. Ras pathway stimulation may alternatively be achieved in HNSCC's by over-expression of membrane bound growth factor receptors, most notably the ErbB family of receptor tyrosine kinases. The four members of this family (ErbB1–4) are commonly over-expressed in HNSCC's and are associated with activation of several major cancer associated signaling cascades including signal transducers and activators of transcription (STAT's), Ras/RAF/MEK/Erk (MAP Kinase), and PI3 Kinase/AKT(Ford and Grandis 2003). ErbB2 specifically is over-expressed in up to 47% of HNSCC's(Cavalot et al 2007), and when combined with expression of E6/E7 causes invasive growth in primary oral keratinocytes, although the mechanism of HPV/ErbB2 synergy and the contribution of the E6 PDZBM were not explored (Al Moustafa et al 2004).

Therefore, we have investigated if the common HNSCC oncogene ErbB2 synergizes with HPV 16 E6 induced PTPN13 loss to result in invasive growth in vivo. To understand how

PTPN13 loss alters cell signaling promoting invasion, we investigated the phosphorylation status of relevant effector pathway signaling components in the presence or absence of functional PTPN13. We describe a mechanism of PTPN13's phosphatase: the regulation MAP Kinase cascade signaling. Furthermore, we provide evidence that PTPN13 loss of function may play a crucial role in potentiating MAP Kinase cascade signaling downstream of multiple different Ras activating oncogenes found in both HPV positive and negative epithelial cancers.

RESULTS

ErbB2 synergizes with PTPN13 loss allowing invasive growth in vivo

Previously, we have shown H-Ras^{v12} expression synergizes with HPV 16 E6 or shRNA mediated PTPN13 loss to allow invasive growth (Spanos et al 2008b). Here, we sought to determine if ErbB2, a common HNSCC oncogene which activates Ras, would also cause invasive growth when PTPN13 is absent. In human cancers, ErbB2 over-expression is oncogenic, but in rodent cancer models activating mutations are required for efficient tumor formation (Moasser 2007). We therefore cloned mouse ErbB2 cDNA into a retroviral vector and performed site directed mutagenesis to introduce a transmembrane region point mutation (ErbB2 V660E) corresponding to that present in a constitutively active rat ErbB2 mutant (neuNT) (Moasser 2007). Previously described MTE cell lines stably expressing HPV16 E6, HPV16 E6 $_{146-151}$, or shPTPN13 (Hoover et al 2007, Spanos et al 2008b) were then transduced with the ErbB2 V660E expression construct. E6 $_{146-151}$ is a deletion mutant of HPV16 which degrades p53 but lacks a PDZ binding motif and does induce loss of PTPN13(Spanos et al 2008b). The shPTPN13 cells lack PTPN13 due to an shRNA mechanism (Spanos et al 2008b). Through western blot, we confirmed that retroviral transduction with ErbB2 V660E increases total and phosphorylated ErbB2 as compared to the parental cells (Figure 1a). Previously described PTPN13 levels (Spanos et al 2008b) were not altered by addition of ErbB2 V660E (not shown).

To determine if HPV 16 E6 PDZBM mediated degradation of PTPN13 is required for invasive growth in synergy with ErbB2, we injected 1×10^6 cells from each ErbB2 V660E expressing cell line subcutaneously into the right, hind legs of C57BL/6 mice (5 mice per group). Weekly caliper measurements were used to calculate average mouse leg circumferences and estimate tumor growth rates over time (Figure 1b). All mice receiving MTE HPV 16 E6/ErbB2 V660E or MTE shPTPN13/ErbB2 V660E cells formed tumors and met criteria for euthanasia within 50 and 30 days, respectively, but no mice receiving MTEHPV 16 E6 $_{146-151}$ /ErbB2 V660E cells showed signs of tumor formation for more than 80 days (Figure 1c). Representative mouse legs from each group are shown at two weeks post-injection (Figure 1d). MTE cells expressing both HPV 16 E6 and E7, and ErbB2 V660E formed tumors at the similar rate as HPV 16 E6/ ErbB2 V660E (data not shown). Thus, oncogenic forms of ErbB2 (Figure 1) and H-Ras (Spanos et al 2008b) synergize with HPV 16 E6 in a similar PDZBM-dependent manner, suggesting that growth factor receptor mediated Ras activation may be important to allow invasive growth in HPV related HNSCC's.

PTPN13 loss correlates with increased Erk phosphorylation

Our in vivo findings show expression of ErbB2 V660E or H-Ras^{V12} is tumorigenic in oropharyngeal keratinocytes only if PTPN13 levels are decreased in parallel, suggesting a potential role for PTPN13 in regulation of cancer signaling pathways affected in common by both ErbB2 and its downstream effector, Ras. To assess what common signaling pathways are altered by loss of PTPN13 and Ras/ErbB2 expression, we examined phosphorylation levels of Erk and AKT. MTE HPV 16 E6 $_{146-151}$/H-Ras^{v12}, MTE HPV 16 E6/ H-Ras^{v12}, and MTE shPTPN13/ H-Ras^{v12} cells were grown to confluency, serum starved for 24 h, and protein lysates collected for immunoblot. Although we observed variation in phospho-AKT levels among the MTE cell lines, we found no correlation between phospho-AKT levels, in vivo invasive growth potential, and the presence/absence of PTPN13. However, cell lines with decreased PTPN13 showed increased levels of phospho Erk1/2 (Figure 2a), a finding which correlates with tumor forming ability in vivo. MTE cells expressing ErbB2 V660E showed similar results (Figure 2b). Immunohistochemistry of mouse tumor samples demonstrated increased levels of phospho-Erk compared to overlying normal epithelium. A representative MTE shPTPN13 ErbB2 V660E tumor is shown in Figure 2c. We also examined phospho-Erk levels in primary human tonsil epithelial (HTE) cells and those expressing combinations of HPV 16 E6, HPV 16 E6 $_{146-151}$, E7, and H-Ras^{v12}, as well as in one HPV 16 positive (UPCI- SCC 90) and one HPV negative (UMSCC 84) head and neck squamous cell carcinoma cell line. In previous work, we have shown UMSCC90 cells have decreased PTPN13 levels compared to UMSCC84 (Spanos et al 2008b). Consistent with our findings in the mouse, HTE cells expressing E6 $_{146-151}$ and E7 showed decreased phospho-Erk levels compared to cells expressing wild type E6 and E7. The addition of H-Ras^{V12} further increased phospho-Erk levels. Moreover, UPCI-SCC90 cells show increased phospho-Erk compared to HTE primary cells. Interestingly, the HPV negative UMSCC84 cell line also showed elevated phospho-Erk, although to a lesser degree than UPCI-SCC90. These findings in human and mouse cells suggest that induced loss of PTPN13 in conjunction with Ras activation permits potentiation of signaling through the MAP kinase pathway.

PTPN13 attenuates MEK and Erk phosphorylation

To further study the role PTPN13 plays in regulating growth factor receptor mediated signaling, we performed co-transfection experiments in HEK 293 cells and examined MAP Kinase cascade signaling in response to PTPN13 status, postulating that if loss permits enhanced signaling then replacement of PTPN13 should suppress signaling. Cells were split to equal, subconfluent densities and co-transfected as indicated with mammalian expression vectors for human PTPN13, ErbB2 (wild type), EGFR (ErbB1), H-Ras^{V12}, or an empty vector control. Following 24 h of serum starvation, protein lysates were collected and vector expression confirmed by immunoblot. As expected, transfection with ErbB2, H-Ras^{V12}, or EGFR, as compared to empty vector control conditions, increased levels of phospho-Erk, which was inhibited by co-expression of PTPN13 (Figure 3). We observed a similar change in phospho-MEK, the immediate upstream activator of Erk. Interestingly, Phospho-AKT levels were not increased by transfection with Ras/ErbB2/EGFR or inhibited by PTPN13 (Figure 3). Since a previous report showed PTPN13 may dephosphorylate ErbB2 directly (Zhu et al 2008), we also examined levels of phospho-ErbB2 (tyr 1248), and we also

observed a small effect in the presence of wild-type PTPN13 (Figure 4). These findings show that under serum starved conditions, PTPN13 consistently attenuates MEK 1/2 and Erk 1/2 phosphorylation in response to activation by various oncogenes common in cervical and/or head and neck cancers.

The phosphatase activity of PTPN13 is required to attenuate MAP Kinase activation

Apart from its phosphatase, PTPN13 has many domains likely important for localization, binding potential substrates, or possibly regulatory roles (Erdmann 2003). The functional significance of the phosphatase domain's in preventing transformation has not been demonstrated. In fact, PTPN13 phosphatase domain null mice show only minor phenotypic defects (Nakahira et al 2007, Wansink et al 2004). Contrary to this transgenic mouse data, a recent screen of colorectal cancers suggests loss of phosphatase function may promote cancer because phosphatase domain mutations frequently co-occurred with mutations in the Ras/MAP Kinase cascade (Wang et al 2004). To determine if PTPN13 phosphatase activity regulates MAP Kinase signaling, we performed site directed mutagenesis to create a phosphatase dead PTPN13 construct for use in our co-transfection studies. An identical mutation resulting in a phosphatase domain cysteine to serine substitution (PTPN13 C2389S) has been shown to abolish PTPN13 catalytic activity (Dromard et al 2007). We repeated the HEK 293 transfection assay with expression vectors for EGFR/ErbB2 and either wild type or C2389S PTPN13 constructs. Immunoblot analysis shows a phosphatase domain function of PTPN13 is necessary to inhibit MAP Kinase signaling in the presence of ErbB2 or EGFR as evidenced by increased levels of phospho-Erk and phospho-MEK in PTPN13 C2389S conditions compared to wild type PTPN13 (Figure 4).

Mutations in HPV negative HNSCC's do not attenuate MAP kinase signaling

The above findings support the hypothesis that loss of PTPN13 phosphatase activity is instrumental in oncogenic signaling. To examine whether HPV negative human tumors demonstrate alternative ways to abrogate PTPN13 enzymatic function we sequenced PTPN13 exons 44–48 (encoding the PTP domain) from 10 HPV negative, human HNSCC specimens. Two patients showed a total of 4 mutations in the coding sequence (one patient had three). This percentage (20%) compares well with that observed in colorectal cancers (9%) (Wang et al 2004). The mutations were cross matched with known SNP's to rule out common polymorphisms and aligned with the protein sequence to determine in which domains the mutations occurred. HNSCC 132 contained one mutation in exon 45, (6874C>T P2276S), and two mutations in exon 46 (7271C>T P2408L and 7316T>C L2423P). HNSCC 134 contained one mutation (c.7205C>T T2386I) in exon 46. The mutations occurring in exon 46 were either within, or close to, important phosphatase domain functional groups (the phosphatase domain binding loop or WPD loop). Therefore, we chose to determine if these mutations affect PTPN13 phosphatase activity and prevent MAP kinase potentiation in conjunction with wild type, human ErbB2. We performed site directed mutagenesis to create corresponding mutations in our PTPN13 expression construct and assessed the PTP activity of immunopurified P2408L and L2423P mutant proteins using DifMUP as an artificial substrate from HNSCC 132. Results indicated that, as compared to wild type PTPN13, both mutants from HNSCC 132 behaved like the catalytically dead C2389S PTPN13 version (Supp. Figure 1). We also repeated the transfection assay in HEK 293 cells and two of the

three mutants, one from each HNSCC, did not reduce levels of phospho-Erk 1/2 (Figure 5b). The result of phospho-Erk 1/2 inhibition do not correspond with the DifMUP phophatase activity because the P2408L mutant does not show activity but is able to inhibit Erk phosphorylation. An examination of phospho-Erk levels, by immunohistochemistry, in the human cancers from which the mutations were isolated showed focal areas of dense staining compared to little/none in normal tonsillar epithelium (Figure 5c). Many of the HNSCC samples without phosphatase domain mutations also showed increased levels of phospho-Erk (data not shown), indicating there may be multiple mechanisms through which MAP Kinase activity is increased in HNSCC's. Our findings suggest PTPN13 phosphatase domain mutations are one mechanism through which increased MAP Kinase activity occurs in HNSCC's.

MEK inhibition by U0126 abrogates Erk phosphorylation and anchorage independent growth in tumorigenic cell lines that have lost PTPN13

Impaired PTPN13 phosphatase activity in HNSCC's may alter signaling cascades other than the MAP kinase pathway. To determine the importance of MAP Kinase signaling for the tumorigenic process and assess the possible therapeutic potential of our findings, we examined levels of phospho-Erk 1/2 in response to the MEK inhibitor U0126 in two tumorigenic cell lines: a cell line derived from a mouse tumor generated by injection with MTE E6E7/ErbB2 V660E cells, and the MTE shPTPN13/ErbB2 V660E cells characterized above. For both cell lines, treatment with increasing doses of U0126 correlated with decreasing levels of phospho-Erk (Figure 6a). To determine the physiological significance of decreased Erk phosphorylation, we examined anchorage independent growth (AIG) colony forming efficiencies during U0126 treatment. Anchorage independent growth correlates with invasive potential in vivo(Reddig and Juliano 2005, Zhan et al 2004), and we have previously shown a correlation between PTPN13 loss and AIG in both mouse and human cell lines(Spanos et al 2008a, Spanos et al 2008b). In the cell lines examined, colony forming efficiencies decreased in a dose dependent response to U0126 that correlates with a decrease in phospho-Erk (Figure 6b). These studies provide evidence that HPV 16 related cancers are dependent on enhanced MAP Kinase signaling during invasive growth and pharmacological inhibition at the level of MEK may serve as a useful therapy.

DISCUSSION

The conversion of a normal epithelial cell to a malignant one requires multiple cellular alterations (Hahn and Weinberg 2002). Our findings show that loss of enzymatic activity of a key phosphatase (PTPN13) synergizes with aberrant MAP Kinase signaling resulting from hyperactivity of epithelial oncogenes like ErbB2 and H-Ras to allow invasive growth in vivo. Importantly, this synergy in potentiating malignant growth is relevant both for HPV positive as well as HPV negative tumors.

Our data strongly suggests HPV 16 mediated PTPN13 loss synergizes with ErbB2 activity during invasive growth in HPV related head and neck cancers, a finding which expands on several previously published reports. ErbB2 and H-Ras have previously been known to synergize with E6 and E7 to allow invasive growth (Al Moustafa et al 2004, Schreiber et al

2004). And, ErbB2/EGFR over-expression occurs in a large proportion of cervical cancers (Perez-Regadera et al 2009), the majority of which are HPV positive. We show that the HPV 16 E6 PDZBM degrades PTPN13 and this induced loss is needed to synergize with ErbB2. The site(s) where PTPN13 acts to exert this control on MAP kinase signaling is still not clear. Using an independent experimental system, Zhu et al have shown PTPN13 physically associates with and decreases phosphorylation of ErbB2 at phosphotyrosine 1248, and that PTPN13 loss enhances carcinogenic signaling downstream of ErbB2 (Zhu et al 2008). Our findings are largely in agreement in that we also show an effect on ErbB2 mediated signaling at the level or MEK and Erk in response to PTPN13 and also showed a change in ErbB2 phosphorylation at tyrosine 1248 that correlated with PTPN13 status. The fact that both ErbB2 and H-RasV12 were potentiated by PTPN13 loss and PTPN13 inhibited MAP kinase signaling downstream of multiple oncogenes (ErbB2, EGFR, H-RasV12), suggest that the phosphatase target that inhibits MAP kinase signaling may not only be limited to ErbB2 tyrosine 1248.

Taken together, the above findings suggest a mechanism of how PTPN13 loss of function synergizes with MAP Kinase activating oncogenes to promote invasive growth across both HPV positive and negative epithelial cancers. Our identification of non-functional PTPN13 mutants that allow aberrant MAP Kinase signaling in HPV negative HNSCC specimens is consistent with studies correlating PTPN13 phosphatase domain mutations in colorectal cancers with alterations in the Ras/MAP Kinase cascade (Wang et al 2004). Also, mounting evidence points to PTPN13 as a potential tumor suppressor in a broad range of other epithelial cancers, including breast, cervical, gastric, and hepatocellular carcinomas (Revillion et al 2009, Wang et al 2004, Yeh et al 2006, Ying et al 2006) There is still some question as to what domain of PTPN13 is required for MAP kinase inhibition. We show some evidence that did not show a correlation between phosphatase activity of a mutant and its ability to inhibit Erk phosphorylation. Mutation P2408L showed very little phosphatase activity by DifMUP assay, yet when transfected with ErbB2 is able to inhibit MAP kinase phosphorylation the same as wild-type. This finding could be explained by a difference in enzymatic specificity for the native substrate versus the artificial DifMUP assay. An alternative explanation is that other domains of the phosphatase are important in forming a possible complex to inhibit MAP Kinase signaling. The mechanism of inhibition and the binding partners involved will be the focus of future studies..

While we have shown a specific synergy with H-RasV12 and ErbB2 in vivo, our findings demonstrate PTPN13 loss likewise alters signaling of EGFR, another common epithelial oncogene. Other receptor tyrosine kinases or pathways that activate MAP kinase signaling may also synergize with PTPN13 disruption during invasive growth. Besides the three examined in this study, a number of MAP Kinase activating oncogenes/mutations have been reported in cancer types known to have decreased or mutated PTPN13. Examples include ErbB3 in the head and neck (Ford and Grandis 2003), RAF in colorectal (Barault et al 2008, Wang et al 2004), and insulin like growth factor receptor (IGFR) and RAF in hepatocellular carcinomas (Avila et al 2006, Hopfner et al 2008),. While our findings provide some insight regarding the role of PTPN13 in MAP kinase signaling, many questions remain unanswered such as what is the target of the phosphatase and what are the roles of the non-phosphatase

domains. (Abaan and Toretsky 2008, Erdmann 2003)Future work will be required to better understand the complete mechanism of suppression.

From a clinical perspective these findings provide rationale for development of better targeted therapies in cancers that have lost PTPN13 function. HPV related cancers, in particular, offer a distinct opportunity for such therapies since the viral oncogenes can be rapidly identified in clinical tumor samples and are associated with consistent changes in cell signaling pathways. It would also be possible to test which tumors have synergizing oncogenes that potentiate MAPK signaling. We have shown that Erk phosphorylation and anchorage independent growth in cells lacking PTPN13 can be inhibited at the level of MEK with U0126, however, U0126 has been shown to be ineffective in vivo, likely due to poor solubility/bioavailability (Wang et al 2007). Clinical trials have been undertaken for MEK inhibitors that show greatly improved pharmacological properties in vivo compared to U0126 (Adjei et al 2008, Lorusso et al 2005, Rinehart et al 2004). These new pharmacological MEK inhibitors may have utility in improving outcomes in HPV related cancers.

METHODS

Retroviral Constructs and Site Directed Mutagenesis

The following mammalian expression vectors were used in transfection experiments: pQCXIX (empty vector) (Clontech), pcDNA3.1 (empty vector), pCMV5-PTPN13(a gift from Ze'ev Ronai), pcDNA3.1-ErbB2, pBabe Puro-H-Ras^{v12}, pBabe Puro-EGFR (Addgene plasmid 11011). Methods for creating the activated mouse ErbB2 retroviral construct (pQCXIH-ErbB2 V660E) and the PTPN13 mutant constructs are described in supplemental methods.

Retroviral Transduction and Selection

Mouse tonsil epithelial (MTE) cell lines stably expressing HPV 16 E6/E7, E6, E6 $_{146-151}$, or shPTPN13 have been described previously and were routinely cultured in E-Media (Hoover et al 2007, Spanos et al 2008b). Retroviral transduction with pQCXIH-ErbB2 V660E was performed using standard methods (Hoover et al 2007). Cell lines were selected in E-Media containing 25–100 μg/mL Hygromycin until non-transduced controls had died (approximately 10 days). Following selection, cells were maintained in E-Media with 5 μg/mL Hygromycin.

In Vivo Invasive Growth

Experiments were carried out as has been previously described (Hoover et al 2007, Spanos et al 2008b). Examination of these tumors by a pathologist demonstrated invasive growth into muscle and capillary/lymphatic growth as was seen in our past model (Spanos *et al.*, 2008). In brief, MTE cells were harvested from tissue culture plates using trypsin (0.25%), and resuspended at 10^3 cells/μL in E-Media. Using an 18-gauge needle, 100 μL of cell suspension was injected subcutaneously in the right, hind leg of each C57BL/6 mouse. Leg circumference was estimated by weekly caliper measurements and using the equation: Circumference=$\pi(3(a+b)-[(a+3b)\times(3a+b)]^{1/2})$, where a is longest leg dimension, and b the

shortest. Mice were humanely euthanized once tumors reached 2 cm in greatest dimension, or the animal became emaciated or had functional leg impairment. An 80-day survival study of 20 mice in four equally sized groups was analyzed using the log rank test with Kaplan-Meier estimated survival functions (Figure1c). The one mortality in the E6 group was related to a non-tumor related anesthesia death. This is indicated in the survival graph.

Cell Lysis and Immunoblot

Cell Lysis and immunoblot analyses were carried out as described previously(Hoover et al 2007). Blots were developed on Kodak® Biomax™ MR film using SuperSignal® West Pico and Femto Chemiluminescent Substrates (Pierce Biotechnology, Rockford, Ill). The following antibodies were used: Anti Fap-1 (Santa Cruz Biotechnology, sc-15356), Anti GAPDH (Ambion, AM4300), Anti Phospho-AKT1/PKB$_\alpha'$ (ser 473) (Upstate, 05–669), Anti Phospho-p44/42 MAPKinase (thr202/204) (Cell Signaling, #9101), Anti Phospho-erbB2 (tyr 1248) (Upstate, 06–229), Anti MapKinase Erk1/Erk2 (Calbiochem, 442704), Anti AKT/PKB (Upstate, 05–591), Anti Phospho-MEK1/2 (ser217/221) (Cell Signaling, #9154), and Anti Human-c-erbB2 oncoprotein (DakoCytomation, A 0485).

Transfection Assay

HEK 293 cells were routinely cultured in Dulbecco's Modified Eagle Medium (DMEM) supplemented with 10% Fetal Bovine Serum and 1% penicillin/streptomycin. Twenty-four h prior to transfection, cells were split and plated at 6×10^6 cells/10 cm plate. Co-transfections were performed per manufacturer instructions using Polyfect® (Qiagen 301105) and 4 μg of each indicated plasmid. Twenty-four hours post-transfection, plates were washed twice with phosphate buffered saline and serum starved for 16–24 h in DMEM before protein lysis.

Anchorage Independent Growth Assay and MEK Inhibitor (U0126) Studies

U0126 (Cell Signaling #9903) was solubilized in dimethylsulfoxide at 8 mg/mL before being added to DMEM at indicated concentrations. To create the MTE E6E7 ErbB2 V660EA tumor cell line, tumor tissue was dissected from the leg of a freshly euthanized, male C57BL/6 mouse injected three weeks prior with MTE E6E7 ErbB2 V660E cells. Tissue was finely minced using a scalpel and subsequent treatment with Dispase II. Cells were cultured using previously described methods(Hoover et al 2007). Indicated amounts of U0126 was applied to the cells in EMEM for 48 h prior to lyses and subsequent immunoblots.

Anchorage independent growth assays were performed by applying a 100 μL base layer of one percent noble agar to 12 mm Transwells® with 0.4 μM polyester membrane inserts (Corning #3460) and allowed to solidify at 4 °C. Cells were suspended at 2×10^3 cells/mL in a mixture of 0.33% noble agar and E-Media at 37 °C. 500 μL of this suspension was added in triplicate to Transwells® and allowed to harden 5 min at 4 °C. Transwells® were added to sterile, twelve-well tissue culture plates containing enough growth media to cover the 1% agar layer (approximately 1.5 mL). Media was changed every other day and supplemented with U0126 at indicated concentrations. Cells were grown in suspension for 17 days. Colonies reaching diameters of 100 μm or greater were counted. AIG percent colony

forming efficiency was determined using the equation: (AIG colonies/cells seeded) $\times$ 100. Anova statistical analysis was used to calculate significance.

Patient Samples

Formalin fixed paraffin embedded oropharyngeal squamous cell carcinoma cases and tonsil tissues from tonsillectomies were obtained from the Department of Pathology archives at University of Iowa Hospitals and Clinics (UIHC). This study was approved by the Institutional Review Board of the University of Iowa. To enrich the amount of DNA collected from tumor cells for PCR and sequencing, grossly visible tumor was isolated from surrounding normal tumor by macrodissection.

Immunohistochemistry

Formalin-fixed, paraffin-embedded tissues were deparaffinized in xylene, antigen unmasked in citrate buffer, and endogenous peroxidases quenched with 2% H2O2. Tissues were blocked with 10% bovine serum albumin. PTPN13 was detected using sc-1138 (Santa Cruz Biotechnology), total ERK1/2 was detected using 4695 and p-ERK1/2 was detected using 4370 (Cell Signaling, Danvers, MA). Incubation with primary antibody (1:125 for PTPN13, 1:1000 for total ERK1/2, 1:400 for p-ERK1/2) was performed overnight at 4 °C. Secondary antibody incubation and detection were carried out with the LSAB+ system (for sc-1138) or EnVision+ system (for 4695, 4370) according to manufacturer's instructions (DakoCytomation). Slides were co-stained with hematoxylin. Blocking peptide (PTPN13, ERK1/2) or secondary antibody (p-ERK) alone controls were completed to validate antibody specificity.

PTPN13 sequencing

Exons 44–48 of PTPN13, were amplified from genomic DNA using PCR. The conditions for the PCR reactions are described in the supplemental methods. PTPN13 mutations were analyzed for significance using several methods. Each mutation was compared to a list of known PTPN13 SNPs using the NCBI and Ensembl databases (www.ncbi.nlm.nih.gov, www.ensembl.org). Sequence conservation among 10 amniotic vertebrates was analyzed using Ensembl's GeneSeqAlignView (www.ensembl.org). PTP amino acid conservation was analyzed using an alignment of 5 PTP's(Villa et al 2005). BLOSUM scores were calculated using a BLOSUM matrix. Each mutation was analyzed for functional consequence using SIFT technology (blocks.fhcrc.org). The location of each mutation within the phosphatase domain was identified using available crystal structure data(Villa et al 2005).

Supplementary Material

Refer to Web version on PubMed Central for supplementary material.

ACKNOWLEDGEMENTS

REFERENCES

Abaan OD, Toretsky JA. PTPL1: a large phosphatase with a split personality. Cancer metastasis reviews. 2008; 27:205–214. [PubMed: 18265946]

Adjei AA, Cohen RB, Franklin W, Morris C, Wilson D, Molina JR, et al. Phase I pharmacokinetic and pharmacodynamic study of the oral, small-molecule mitogen-activated protein kinase kinase 1/2 inhibitor AZD6244 (ARRY-142886) in patients with advanced cancers. J Clin Oncol. 2008; 26:2139–2146. [PubMed: 18390968]

Al Moustafa AE, Foulkes WD, Benlimame N, Wong A, Yen L, Bergeron J, et al. E6/E7 proteins of HPV type 16 and ErbB-2 cooperate to induce neoplastic transformation of primary normal oral epithelial cells. Oncogene. 2004; 23:350–358. [PubMed: 14724563]

Avila MA, Berasain C, Sangro B, Prieto J. New therapies for hepatocellular carcinoma. Oncogene. 2006; 25:3866–3884. [PubMed: 16799628]

Barault L, Veyrie N, Jooste V, Lecorre D, Chapusot C, Ferraz JM, et al. Mutations in the RAS-MAPK, PI(3)K (phosphatidylinositol-3-OH kinase) signaling network correlate with poor survival in a population-based series of colon cancers. International journal of cancer. 2008; 122:2255–2259.

Cavalot A, Martone T, Roggero N, Brondino G, Pagano M, Cortesina G. Prognostic impact of HER-2/neu expression on squamous head and neck carcinomas. Head Neck. 2007; 29:655–664. [PubMed: 17315173]

Dromard M, Bompard G, Glondu-Lassis M, Puech C, Chalbos D, Freiss G. The putative tumor suppressor gene PTPN13/PTPL1 induces apoptosis through insulin receptor substrate-1 dephosphorylation. Cancer Res. 2007; 67:6806–6813. [PubMed: 17638892]

Erdmann KS. The protein tyrosine phosphatase PTP-Basophil/Basophil-like. Interacting proteins and molecular functions. Eur J Biochem. 2003; 270:4789–4798. [PubMed: 14653806]

Ford AC, Grandis JR. Targeting epidermal growth factor receptor in head and neck cancer. Head Neck. 2003; 25:67–73. [PubMed: 12478546]

Hahn WC, Weinberg RA. Rules for making human tumor cells. N Engl J Med. 2002; 347:1593–1603. [PubMed: 12432047]

Hanahan D, Weinberg RA. The hallmarks of cancer. Cell. 2000; 100:57–70. [PubMed: 10647931]

Hardisson D. Molecular pathogenesis of head and neck squamous cell carcinoma. Eur Arch Otorhinolaryngol. 2003; 260:502–508. [PubMed: 12736744]

Hoover AC, Spanos WC, Harris GF, Anderson ME, Klingelhutz AJ, Lee JH. The role of human papillomavirus 16 E6 in anchorage-independent and invasive growth of mouse tonsil epithelium. Arch Otolaryngol Head Neck Surg. 2007; 133:495–502. [PubMed: 17515506]

Hopfner M, Schuppan D, Scherubl H. Growth factor receptors and related signalling pathways as targets for novel treatment strategies of hepatocellular cancer. World J Gastroenterol. 2008; 14:1–14. [PubMed: 18176955]

Hsu J. The factor analytic approach to simultaneous inference in the general linear model. J Computational and Graphical Statistics 1, 151 (1992). 1992; 1:151.

Jelen F, Oleksy A, Smietana K, Otlewski J. PDZ domains - common players in the cell signaling. Acta Biochim Pol. 2003; 50:985–1017. [PubMed: 14739991]

Landro ME, Dalbert D, Picconi MA, Cuneo N, Gonzalez J, Vornetti S, et al. Human papillomavirus and mutated H-ras oncogene in cervical carcinomas and pathological negative pelvic lymph nodes: a retrospective follow-up. J Med Virol. 2008; 80:694–701. [PubMed: 18297710]

Lee JH, Lee SK, Yang MH, Ahmed MM, Mohiuddin M, Lee EY. Expression and mutation of H-ras in uterine cervical cancer. Gynecol Oncol. 1996; 62:49–54. [PubMed: 8690291]

Longworth MS, Laimins LA. Pathogenesis of human papillomaviruses in differentiating epithelia. Microbiol Mol Biol Rev. 2004; 68:362–372. [PubMed: 15187189]

Lorusso PM, Adjei AA, Varterasian M, Gadgeel S, Reid J, Mitchell DY, et al. Phase I and pharmacodynamic study of the oral MEK inhibitor CI-1040 in patients with advanced malignancies. J Clin Oncol. 2005; 23:5281–5293. [PubMed: 16009947]

Lu SL, Herrington H, Reh D, Weber S, Bornstein S, Wang D, et al. Loss of transforming growth factor-beta type II receptor promotes metastatic head-and-neck squamous cell carcinoma. Genes Dev. 2006; 20:1331–1342. [PubMed: 16702406]

Moasser MM. The oncogene HER2: its signaling and transforming functions and its role in human cancer pathogenesis. Oncogene. 2007; 26:6469–6487. [PubMed: 17471238]

Nakahira M, Tanaka T, Robson BE, Mizgerd JP, Grusby MJ. Regulation of signal transducer and activator of transcription signaling by the tyrosine phosphatase PTP-BL. Immunity. 2007; 26:163–176. [PubMed: 17306571]

Perez-Regadera J, Sanchez-Munoz A, De-la-Cruz J, Ballestin C, Lora D, Garcia-Martin R, et al. Negative prognostic impact of the coexpression of epidermal growth factor receptor and c-erbB-2 in locally advanced cervical cancer. Oncology. 2009; 76:133–141. [PubMed: 19174612]

Reddig PJ, Juliano RL. Clinging to life: cell to matrix adhesion and cell survival. Cancer metastasis reviews. 2005; 24:425–439. [PubMed: 16258730]

Revillion F, Puech C, Rabenoelina F, Chalbos D, Peyrat JP, Freiss G. Expression of the putative tumor suppressor gene PTPN13/PTPL1 is an independent prognostic marker for overall survival in breast cancer. International journal of cancer. 2009; 124:638–643.

Rinehart J, Adjei AA, Lorusso PM, Waterhouse D, Hecht JR, Natale RB, et al. Multicenter phase II study of the oral MEK inhibitor, CI-1040, in patients with advanced non-small-cell lung, breast, colon, and pancreatic cancer. J Clin Oncol. 2004; 22:4456–4462. [PubMed: 15483017]

Schreiber K, Cannon RE, Karrison T, Beck-Engeser G, Huo D, Tennant RW, et al. Strong synergy between mutant ras and HPV16 E6/E7 in the development of primary tumors. Oncogene. 2004; 23:3972–3979. [PubMed: 15077191]

Spanos WC, Geiger J, Anderson ME, Harris GF, Bossler AD, Smith RB, et al. Deletion of the PDZ motif of HPV16 E6 preventing immortalization and anchorage-independent growth in human tonsil epithelial cells. Head Neck. 2008a; 30:139–147. [PubMed: 17657785]

Spanos WC, Hoover A, Harris GF, Wu S, Strand GL, Anderson ME, et al. The PDZ binding motif of human papillomavirus type 16 E6 induces PTPN13 loss, which allows anchorage-independent growth and synergizes with ras for invasive growth. J Virol. 2008b; 82:2493–2500. [PubMed: 18160445]

Villa F, Deak M, Bloomberg GB, Alessi DR, van Aalten DM. Crystal structure of the PTPL1/FAP-1 human tyrosine phosphatase mutated in colorectal cancer: evidence for a second phosphotyrosine substrate recognition pocket. J Biol Chem. 2005; 280:8180–8187. [PubMed: 15611135]

Wang D, Boerner SA, Winkler JD, LoRusso PM. Clinical experience of MEK inhibitors in cancer therapy. Biochim Biophys Acta. 2007; 1773:1248–1255. [PubMed: 17194493]

Wang Z, Shen D, Parsons DW, Bardelli A, Sager J, Szabo S, et al. Mutational analysis of the tyrosine phosphatome in colorectal cancers. Science. 2004; 304:1164–1166. [PubMed: 15155950]

Wansink DG, Peters W, Schaafsma I, Sutmuller RP, Oerlemans F, Adema GJ, et al. Mild impairment of motor nerve repair in mice lacking PTP-BL tyrosine phosphatase activity. Physiol Genomics. 2004; 19:50–60. [PubMed: 15226483]

Yarbrough WG, Shores C, Witsell DL, Weissler MC, Fidler ME, Gilmer TM. ras mutations and expression in head and neck squamous cell carcinomas. Laryngoscope. 1994; 104:1337–1347. [PubMed: 7968162]

Yeh SH, Wu DC, Tsai CY, Kuo TJ, Yu WC, Chang YS, et al. Genetic characterization of fas-associated phosphatase-1 as a putative tumor suppressor gene on chromosome 4q21.3 in hepatocellular carcinoma. Clin Cancer Res. 2006; 12:1097–1108. [PubMed: 16489062]

Ying J, Li H, Cui Y, Wong AH, Langford C, Tao Q. Epigenetic disruption of two proapoptotic genes MAPK10/JNK3 and PTPN13/FAP-1 in multiple lymphomas and carcinomas through hypermethylation of a common bidirectional promoter. Leukemia. 2006; 20:1173–1175. [PubMed: 16572203]

Zhan M, Zhao H, Han ZC. Signalling mechanisms of anoikis. Histol Histopathol. 2004; 19:973–983. [PubMed: 15168359]

Zhu JH, Chen R, Yi W, Cantin GT, Fearns C, Yang Y, et al. Protein tyrosine phosphatase PTPN13 negatively regulates Her2/ErbB2 malignant signaling. Oncogene. 2008; 27:2525–2531. [PubMed: 17982484]
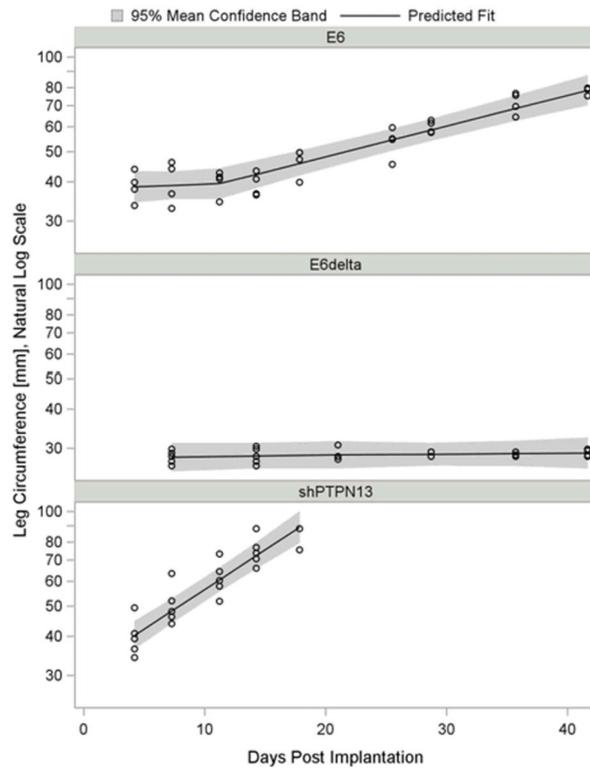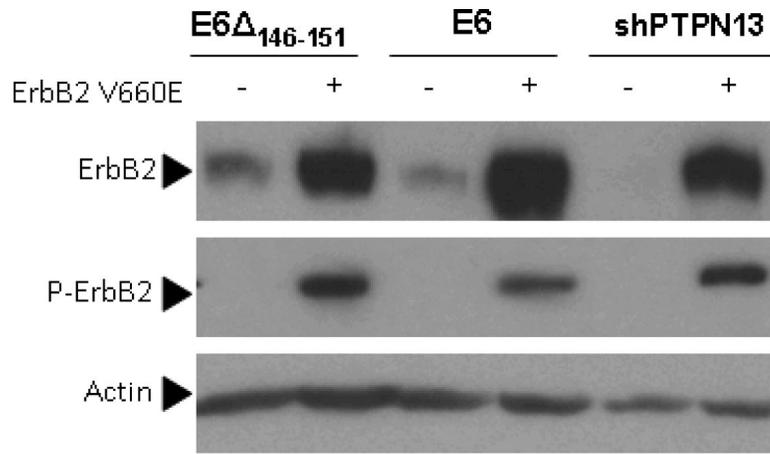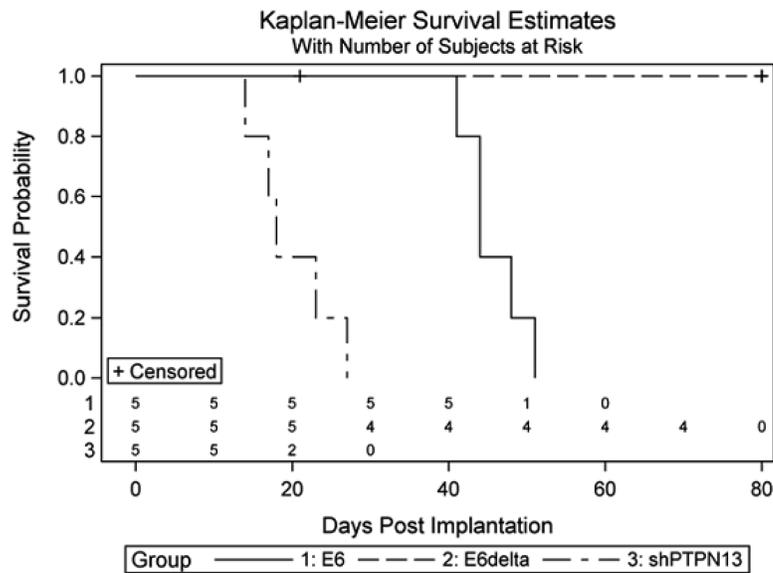
Figure 1. ErbB2 synergizes with PTPN13 loss during invasive growth in vivo
(**a**) MTE cell lines stably expressing HPV 16 E6, E6 $_{146–151}$, or PTPN13 shRNA (shPTPN13) were retrovirally transduced to express activated mouse ErbB2 (ErbB2 V660E). Functional protein expression, as compared to non-transduced cell lines, was confirmed by immunoblot with antibodies to total and phosphorylated ErbB2. Actin immunostaining served as loading control. (**b,c**) One million cells from each line were injected subcutaneously into the right hind legs of C57BL/6 mice (n=5 per group). Mouse leg circumferences and tumor growth rates were calculated based on weekly caliper measurements of leg dimensions, and mice were euthanized once tumors reached 20 mm in

greatest dimension. The three treatment groups were compared to E6 using 2-sided Dunnett adjustment for multiple comparisons developed by Hsu(Hsu 1992). The shPTPN13 and E6 groups were significantly different than the control group (p < 0.0001 and p = 0.009, respectively). The median survival times in the same order of reporting as above were 18, 44 and 80 days, respectively. (**d**) Representative mouse legs from each group are shown at approximately two weeks post injection.
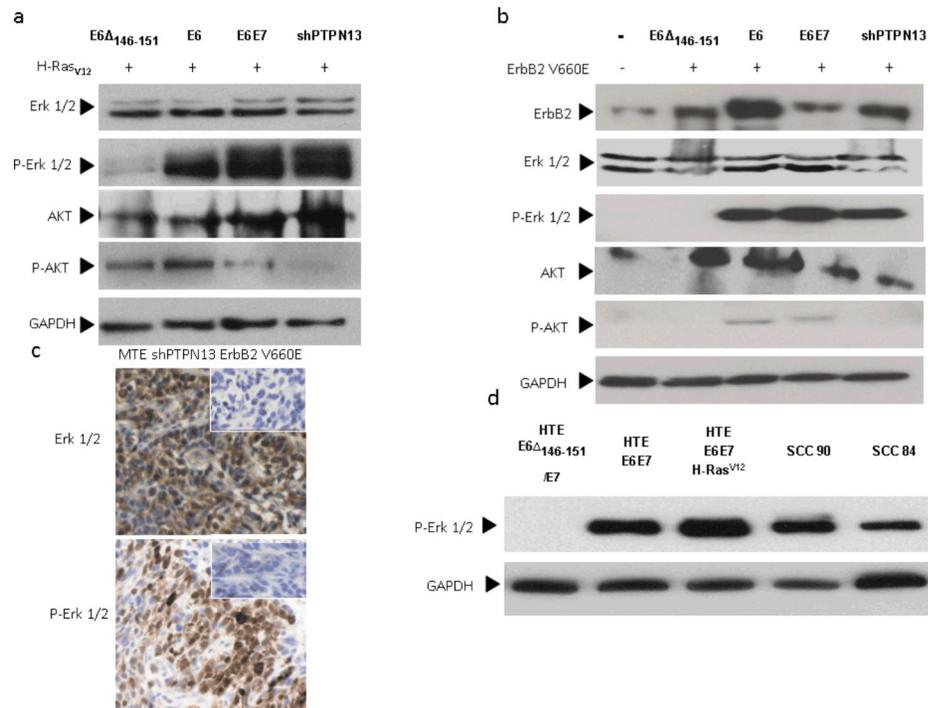
Figure 2. PTPN13 loss correlates with increased Erk 1/2 phosphorylation

(**a,b**) Lysates of serum starved MTE cell lines stably expressing HPV 16 E6, E6 and E7, E6 $_{146-151}$, or PTPN13 shRNA (shPTPN13) as well as H-Ras^{V12} or ErbB2 V660E were subjected to immunoblot analysis with indicated antibodies. (**c**) Immunohistochemistry for total and phosphorylated Erk 1/2 was performed on a representative tumor derived from a mouse implanted with MTE shPTPN13 ErbB2 V660E cells. Insets display control immunostainings of parallel sections to reveal antibody specificity. (**d**) HNSCC cell lines (SCC 90 and SCC 84) as well as human tonsil epithelial (HTE) primary cells or those stably expressing HPV 16 E6, E7, E6 $_{146-151}$, and H-Ras^{V12} as indicated were subject to immunoblot analysis with antibody to phosphorylated Erk 1/2. Immunostaining for GAPDH was performed to monitor equal loading of protein samples.
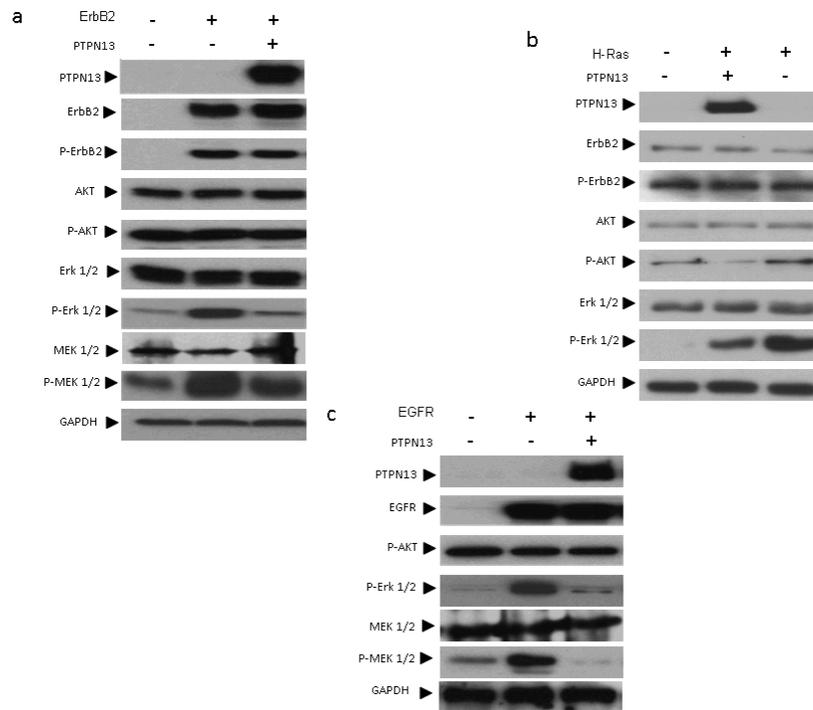
Figure 3. PTPN13 inhibits MAP Kinase cascade signaling
HEK 293 cells were transfected with mammalian expression vectors for (a) ErbB2, (b) H-Ras^{V12}, or (c) EGFR as well as PTPN13 or an equivalent empty vector control. Two days post transfection serum starved cells were lysed and subjected to immunoblot analysis using indicated antibodies. GAPDH immunostaining served as loading control.
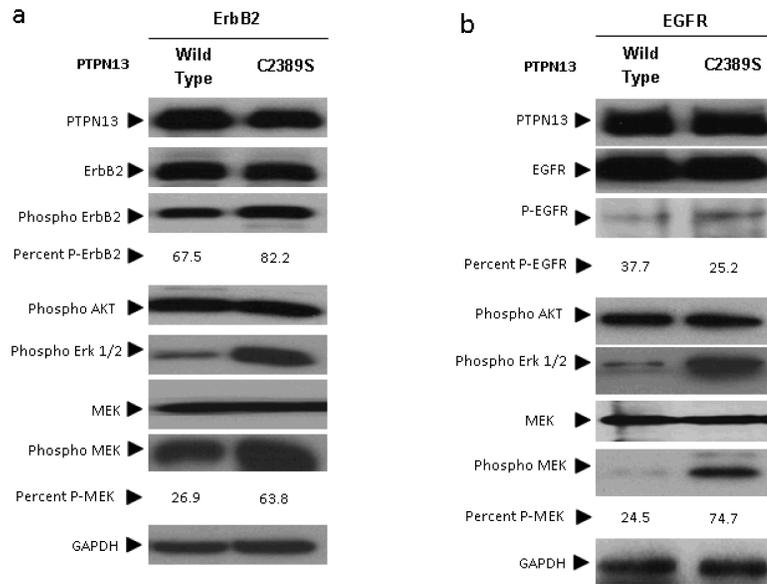
Figure 4. PTPN13's phosphatase activity is required to attenuate MAP Kinase signaling

HEK 293 cells were co-transfected as indicated with (**a**) ErbB2 or (**b**) EGFR and either wild type or phosphatase dead (C2389S) PTPN13 expression constructs. Two days post transfection serum starved cells were lysed, subjected to immunoblot analysis using indicated antibodies and densitometry calculated as described in supplement methods. After transfection with either the wild-type or C2398S the percent phosphorylated MEK, ErbB2 and EGFR is indicated. .
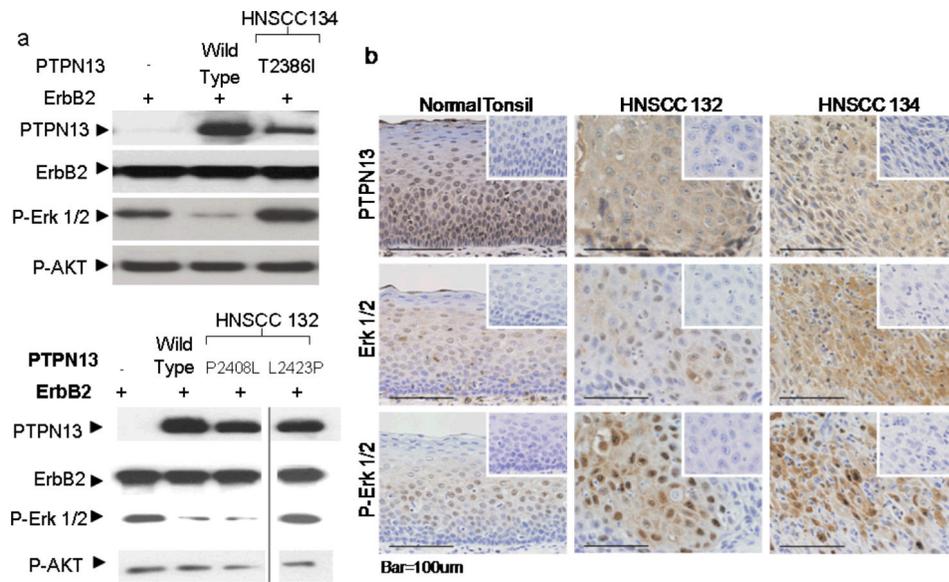
Figure 5. A subset of HPV negative head and neck squamous cell carcinomas harbor PTPN13 phosphatase domain mutations

DNA sequencing of HPV negative, paraffin embedded HNSCC samples revealed phosphatase domain mutations in two out of ten patients. (**a**) HEK 293 cells were co-transfected with ErbB2 and PTPN13 constructs containing phosphatase domain point mutations corresponding to those found in the two HNSCC samples. Cells were serum starved following transfection and immunoblot was performed using indicated antibodies. (**b**) Immunohistochemistry of these two HNSCC samples and of normal tonsil tissue was performed to assess PTPN13 expression and the levels of total and phosphorylated Erk 1/2. Insets display control immunostainings of parallel sections to reveal antibody specificity.
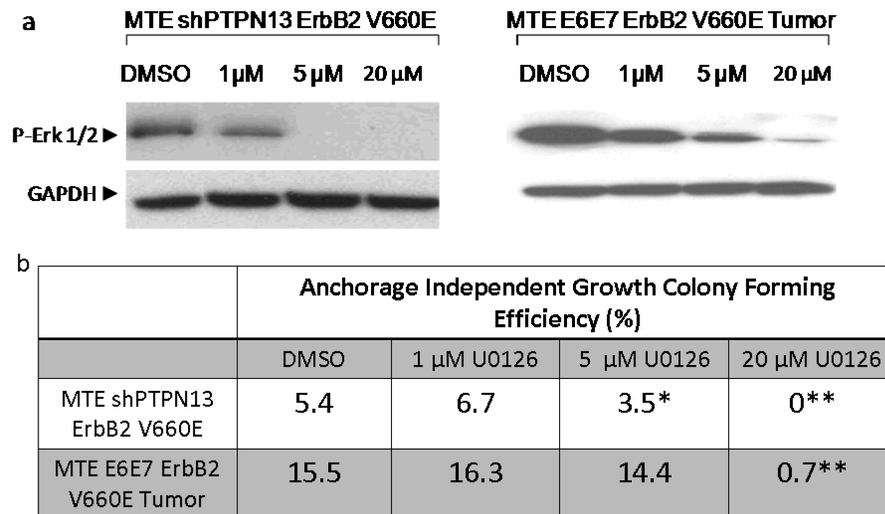
Figure 6. MEK inhibition by U0126 prevents anchorage independent growth in tumorigenic cell lines

(**a**) A cell line derived from a mouse injected with MTE E6E7 ErbB2 V660E cells and MTE shPTPN13 ErbB2 V660E cells were treated for 4 h with 0, 1, 5, or 20 μM U0126 in serum free medium. Levels of phosphorylated Erk 1/2 in the respective lysates were assessed by western blot using GAPDH immunostaining as a loading control. (**b**) The same cell lines were plated in triplicate, suspended in semisolid agar in 12 mm transwells, and fed growth media with indicated concentrations of U0126 for approximately two weeks. Average colony forming efficiencies for each condition are indicated. Significant differences compared to DMSO controls were obtained as indicated (p values of *= 0.002 and **<0.0001).